2008 IEEE International Conference on
Robotics and Automation
Pasadena, CA, USA, May 19-23, 2008

A 200Hz Small Range Image Sensor Using a Multi-Spot Laser Projector

Masateru Tateishi, Hidetoshi Ishiyama and Kazunori Umeda

Abstract— **In this paper, a high-speed range image sensor using a multi-spot laser projector is constructed. Several high-speed range image sensors have been developed recently. Their sampling rate is around the video rate (30Hz or so) and a faster sensor is required. The proposed sensor has achieved 200Hz measurement. It consists of a commercially available laser projector and a high-speed CCD camera. The number of pixels is 361 and the measurement range is 800-2000mm. Although the acquired range image is sparse, the proposed sensor is thought to be adequate for several applications such as robot vision because of its high-speed imaging and compactness. Some characteristics such as measurement errors are discussed, and the effectiveness of the proposed sensor is verified by experiments.**

I. Introduction

Range images are important sensor information for many applications. Many methods to acquire range images have been studied in the field of computer vision, robot vision, optics etc. [1], [2], [3], and several sensors are commercially available now. However, many of them are mainly for precise modeling of objects and not suitable for real-time applications such as robot vision.

Some methods can acquire range images in real time. Stereo vision is the most intensively studied range imaging technique, and a real-time stereo camera is now commercially available [4]. Kanade et al. proposed multi-baseline stereo to increase robustness of stereo vision, and constructed a video rate stereo camera [5]. On the other hand, several active methods have been proposed. Beraldin et al. realized a video rate range imaging by scanning a laser spot using their synchronized laser scanning technique [6]. Sato [7] and Kanade [8] developed a special imaging detector and realized real time imaging by scanning a laser slit with the detector. These active sensors need scanning. Some sensors realized scanless range image measurement by projecting multi-spots [9], [10], [11]. In [9], special spot pattern that is made with a mask and a halogen lamp is projected, and by developing a special hardware, video rate range imaging was realized. In [10], spot pattern was generated by using a fiber grating and a laser. This type of sensor using a fiber grating has been used for some applications such as object recognition [12] and navigation of a mobile robot [13]. Recently, a new technology for range imaging based on the time-of-flight method is emerging, and some sensors are already commercially available [14], [15]. In the sensors, modulated light is projected by infrared LEDs and the time-of-flight range measurement is done simultaneously at each pixel of a special image sensor.

M. Tateishi was with Course of Precision Engineering, School of Science and Engineering, Chuo University, 1-13-27 Kasuga, Bunkyo-ku, Tokyo 112-8551, Japan

H. Ishiyama and K. Umeda are with Department of Precision Mechanics, Faculty of Science and Engineering, Chuo University, 1-13-27 Kasuga, Bunkyo-ku, Tokyo 112-8551, Japan ishiyama@sensor.mech.chuo-u.ac.jp, umeda@mech.chuo-u.ac.jp

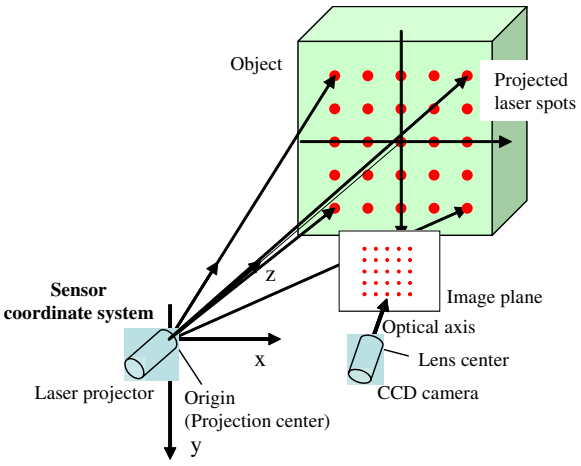

Fig. 1. Structure of the range image sensor using a multi-spot projector

The sampling rate of the above-mentioned real-time sensors are around the video rate (30Hz or so). As for an ordinary image, faster cameras have emerged and given great impacts for several applications such as visual tracking by a robot [16], [17]. Sampling rate of these sensors is as fast as 1kHz. For a range image sensor, such fast imaging is effective, too.

In this paper, we propose a faster range image sensor with the sampling rate of 200Hz, using a multi-spot laser projector.

II. Principle of the Sensor

A. Range image measurement using a multi-spot laser projector

Fig.1 illustrates the structure of the sensor. The structure is similar to [10], [11]. Multiple laser spots are projected by a laser projector, and a scene with projected multi-spots are observed by a CCD camera. The spots in images of the CCD camera are extracted, and for each spot, disparity is measured and distance is calculated by the triangulation.

Position of each point in 3D space can be calculated by a standard stereo method [18]. For this sensor, it is convenient that the coordinate system is set at the projector. When each spot can be assumed to be projected from a same point (which is often the case; hereafter, call the point projection center), it is simple that the origin is attached to

the projection center, and that one axis is set to the direction of projecting the center spot and the other two axes are set parallel to horizontal and vertical directions of the spot array.

Hereafter, we use the word distance as the one measured along the direction of the optical axis (z-axis in Fig.1). The distance is obtained by the following equation.

$$z = \frac{\alpha}{k}, \qquad \alpha = \frac{b \cdot f}{p} \tag{1}$$

b: baseline length (distance between the projection center and the lens center)

f: focal length of the lens of the CCD camera

p: width of each pixel of the image

k: disparity for infinite distance

Note that the unit of k is pixel. To measure the distance with (1), it is not necessary to give b, f, p independently; only α is necessary.

The distance above is the one measured from the lens center of the CCD camera in the direction of the CCD camera's optical axis. When the laser projector and the CCD camera are set parallel and z coordinate of the lens center of the CCD camera is zero, this distance and the one in the sensor coordinate system corresponds. In general, α differs for each spot.

B. Improvement of measurement range by rotation of laser projector

As this sensor uses multi-spots, it is necessary to obtain the correspondence between projected spots and their observed image, i.e., the correspondence problem in the stereo vision has to be solved. We take advantage of a practical method to limit measurement range so that the correspondences become unique, e.g, we assume that the distance is always larger than a certain value. Fig.2(a) illustrates the image of spots. In the image plane, each spot moves on the epipolar line [18] according to the distance. The epipolar lines of the spots in a same row overlap and the spot image cannot be corresponded to the spot uniquely. To achieve the uniqueness of the correspondence, ranges in which spots move in the image need to be restricted so that they have no overlap as shown in Fig.2(a).

We reduce this limitation by rotating the laser projector as shown in Fig.3. Fig.2(b) illustrates the image of spots with the rotation. This figure shows that the ranges in which spots can move without overlap become larger. Consequently, the measurable range of the sensor becomes larger, or with the same measurable range, the precision of measurement can be improved because the number of the pixels assigned to each spot for measuring the same range becomes larger. It can be said that the regions of the image that were originally not used, i.e., regions between epipolar lines, are efficiently used with the rotation.

Note that the rotation angle should not be too small to prevent the failure of correspondence of two adjacent spots.

C. Some characteristics of the sensor

1) Relation of sensor parameters: Let the restriction for measurement range be between z_1 and z_2 ($z_1 < z_2$) and

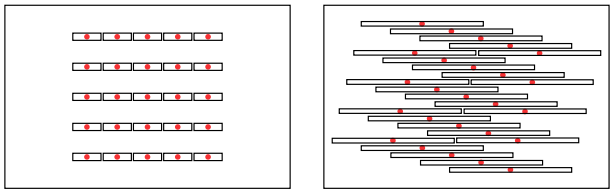

(a)Without rotation (b)With rotation

Fig. 2. Restriction for epipolar line of each spot

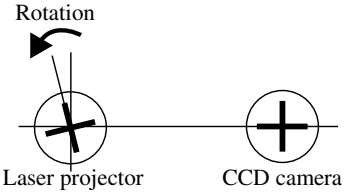

Fig. 3. Rotation of laser projector

the disparity for each distance be k_1 and k_2 respectively. $n \equiv k_1 - k_2$ represents the number of pixels assigned to each spot. From (1),

$$n = k_1 - k_2 = \alpha \left(\frac{1}{z_1} - \frac{1}{z_2} \right) = \frac{b \cdot f}{p} \left(\frac{1}{z_1} - \frac{1}{z_2} \right). \tag{2}$$

When the angle between adjacent spots is given, n can be calculated. Let the angle be $d[rad]$ and the magnification of the number of assigned pixels given in II-B be m. Then

$$n = m \cdot \frac{d \cdot f}{p}. \tag{3}$$

From (2) and (3),

$$b \left(\frac{1}{z_1} - \frac{1}{z_2} \right) = m \cdot d. \tag{4}$$

Parameters of the sensor are related with these equations. p is given when the CCD camera (and a image board for an analog camera) is selected. f is selected by the field of view required to observe the whole spots. And the relation between the measurement range (i.e.,z_1 and z_2) and the baseline length b is given by (4); when z_1 and z_2 are given, the baseline length b is calculated by (4), or when b is given, the measurement range (z_1 or z_2) is calculated.

The brightness of the spot image is in principle inverse proportional to the square of the distance, and z_2 can be limited by the brightness. However, it is safe to set z_2 to infinite so as to reduce the possibility of wrong measurement; if an object has strong mirror reflection, it may reflect the spot directly to the camera and the spot image may become unexpectedly bright even though the object is far away. Therefore, we set z_2 to infinite. Then (4) becomes

$$z_1 = \frac{b}{m \cdot d}. \tag{5}$$

2) Error analysis of range measurement: The position of the spot in the image can be measured with subpixel precision by some techniques such as obtaining the center of the gravity of the spot image. The precision is limited by the laser speckle [19], etc. Let the precision be σ_k. It can roughly be said that distance can be measured with the level of n/σ_k. The precision of measuring distance is derived from (1). By applying the law of propagation of errors,

$$\sigma_z = \frac{1}{\alpha} z^2 \sigma_k \tag{6}$$

where σ_z is the precision of the measured distance. This equation shows that the error of measuring distance is proportional to the square of the distance, which is well known for range measurement with triangulation. By substituting (2) for (6),

$$\sigma_z = \frac{z_2 - z_1}{z_1 z_2} z^2 \frac{\sigma_k}{n}. \tag{7}$$

When z_2 is infinite, (7) becomes

$$\sigma_z = \frac{z^2}{z_1} \frac{\sigma_k}{n}. \tag{8}$$

When $z = z_1$, (8) becomes

$$\sigma_z = z_1 \frac{\sigma_k}{n}. \tag{9}$$

This indicates that the resolution for the nearest distance is obtained by dividing the distance by the number of the level (i.e., n/σ_k).

III. Construction of the sensor

A. Sensor hardware

Fig.4 shows the constructed range image sensor. The laser projector is StockerYale Mini-519X [20]. The wavelength of the laser is 785nm (near infrared) and its power is 35mW. It projects 19×19, totally 361 spots using a diffraction grating attached at the tip of the laser projector. The angle between adjacent spots is 0.90°. The CCD camera is Point Grey Research Dragonfly Express. Its maximum frame rate is 200fps, which is achieved by using fast interface to PC IEEE1394b and PCI Express. The number of pixels is 640×480, and the size of the pixel is 7.4μm^2. A lens with f=8mm is used, and a Hoya R72 optical filter is attached to the lens. The light with the wavelength less than 720nm is cut by the filter, and thus the effect of disturbance light is reduced. The laser projector and the CCD camera are set parallel with the baseline length 47.5mm. The sensor's size is small enough to use for many applications such as a sensor of a mobile robot.

The rotation angle of the projector is $\arctan(1/4) = 14.0°$ as shown in Fig.2(b), which makes magnification of the number of assigned pixels $\sqrt{17}$ times. With this angle, the distance between epipolar lines of two adjacent spots is 4.1pixels and this is free of the failure. Then the number of pixels assigned to each spot n becomes 70 from (3).

Fig. 4. Constructed range image sensor (left: laser projector, right: CCD camera. size: 100mm×70mm×73mm, including the lens)

B. Processing for fast measurement

Images are captured at every 5ms by the CCD camera. To achieve 200Hz range image measurement, image processing has to be done within 5ms. Image processing is done while the CCD camera is capturing the next image.

The position of the spot image is searched on the epipolar line. The epipolar line of this sensor is horizontal, and thus the search can be easily done. To reduce the calculation cost, only one line is searched for each spot image. After thresholding, the center of the gravity is calculated as the position of the spot image. The disparity is obtained from the position, and the distance is calculated with (1). Note that α in (1) should be given for each spot separately. The calculated value of α using given parameters is 51351, and on the other hand, α for each spot obtained by a calibration using a plane set at known distances distributes from 48227 to 55187.

A DELL Dimension8400 PC with Pentium4 3.2GHz and memory 1024MB is used. The total processing time of calculating a range image with this PC is less than 1ms, which is fast enough.

C. Specifications of the constructed sensor

In this section, we show some specifications of the constructed sensor.

1) Measurement range: We set $z_2 = \infty$. Then the minimum measurable distance z_1 becomes about 733mm from (5). By adding some margin, we set the minimum distance to 800mm. And the maximum distance with good measurement was empirically obtained to be about 2000mm. When distance becomes larger, the spot image becomes darker in proportion to the square of the distance and detection of spot image becomes difficult. Consequently, the measurement space of the sensor becomes Fig.5. Spatial resolution, i.e., distance between adjacent spots is 12.6mm at 800mm and 31.5mm at 2000mm.

Robustness to the disturbance light has not been examined precisely. The measurable distance tends to become shorter when the disturbance light becomes brighter. Roughly speaking, indoor measurement with fluorescent lighting is robust, and under direct sunlight, measurement becomes impossible.

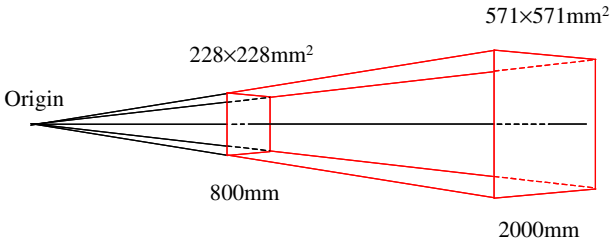

Fig. 5. Measurement space of the sensor

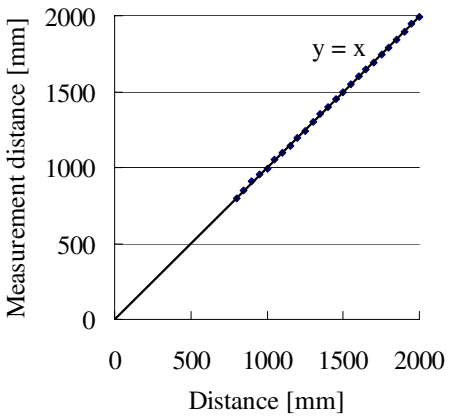

Fig. 6. Relation between the actual and measured distances

2) Precision of range measurement: Fig.6 and Fig.7 show the experimentally obtained precision of measured distances. They represent the average (Fig.6) and the standard deviation (Fig.7) for 361 points at every 50mm distance. It is shown that the distances are appropriately measured without bias and the error of measuring distance is proportional to the square of the distance as given in (6). And using (6), the measurement error of position of spot image σ_k is calculated as 0.225pixel from 4.39E-06 in Fig.7 and the calculated α=51351.

Fig.8 shows the detailed measurement errors around the middle of the measurement range. Each point and error bar represent the average and standard deviation for 361 points at each distance. This result shows in detail that the distances are appropriately measured without bias.

IV. Experiments

A. Examples of range image measurement

We show examples of range image measurement. Fig.9 shows an example of measuring a 200×200×300mm^3 polystyrene block and a 60×120×200mm^3 wooden block. In Fig.9(a), the optical filter is removed to show the objects. Rotated spot images can be seen. Fig.9(b) shows the obtained range image. Although the range image is sparse with only 361 points, rough 3D shape is obtained.

Fig.10 shows another example of measuring a 250mm height doll. Rough 3D shape of the complex object with curved surfaces the is obtained.

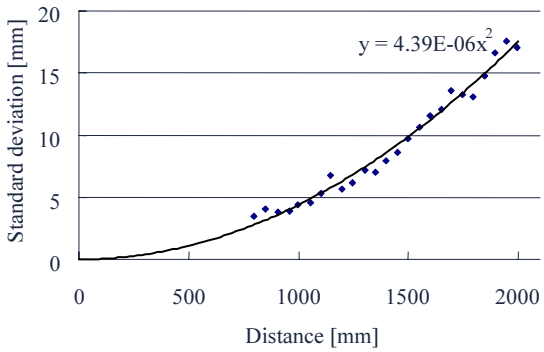

Fig. 7. Standard deviation of the measured distance

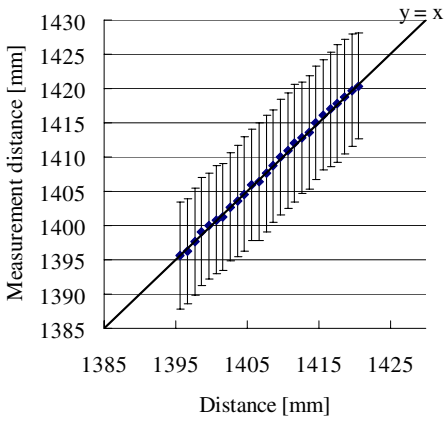

Fig. 8. Relation between the actual and measured distances

B. Verification of 200Hz measurement

Next we show experimental results to verify 200Hz measurement. Fig.11 shows the target image without the optical filter. A soccer ball of diameter about 90mm is suspended by a string and makes a pendulum. The length of the pendulum is about 350mm and its cycle is about 1.2s. Fig.12 shows the measured back-and-forth vibration of the pendulum. The vertical axis represents the distance to the center of gravity of obtained ball range image. Fig.13 shows the magnified figure of Fig.12 between 1.2s to 1.4s. These results show that the vibration motion of the ball is measured well, and the measurement is achieved at every 5ms, i.e., 200Hz is verified.

Fig.14 shows the setup of another experiment. A ball of diameter 70mm was dropped in front of the sensor, and its range images were acquired. The period that the ball was in the field of view of the sensor was about 150ms and 30 range images were acquired. Fig.15 shows continuous two of them (24, 25 frames). The ball speed was about 2.86m/s. Range images are adequately measured at every frame and the change of two range images are small for the rather high speed of ball, and the effectiveness of the fast measurement is shown.

V. Conclusion

In this paper, we have constructed a high-speed range image sensor with the sampling rate of 200Hz, and verified its effectiveness by experiments. It consists of a commer-

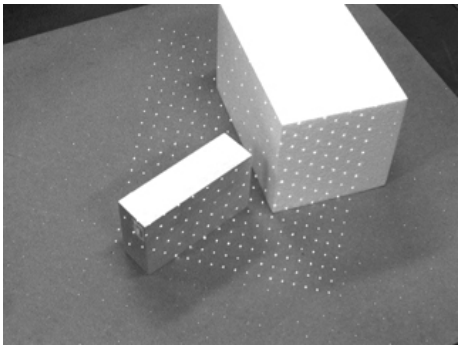

(a)Original image (without R72 filter)

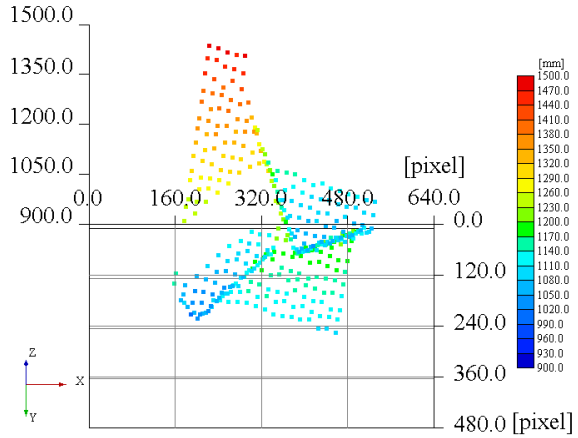

(b)Obtained range image

Fig. 9. Range image of rectangular parallelepipeds

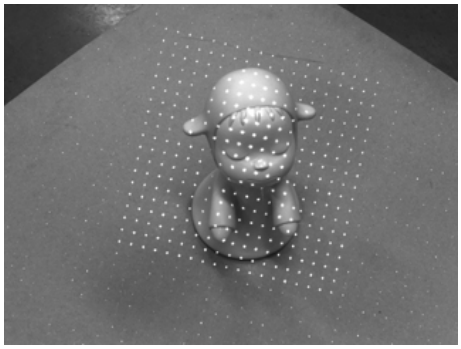

(a)Original image (without R72 filter)

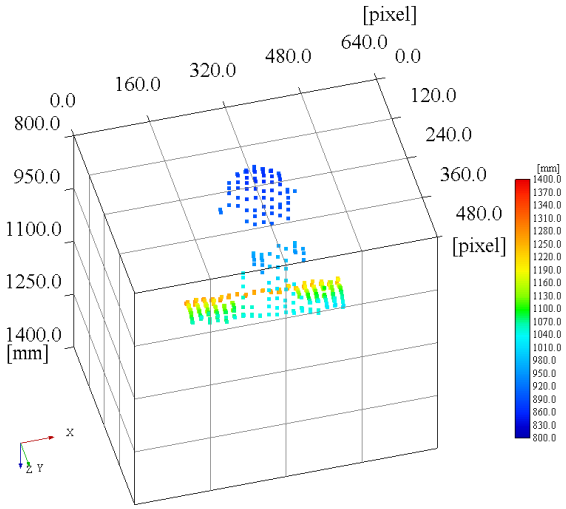

(b)Obtained range image

Fig. 10. Range image of a doll

cially available laser projector that projects multiple spots and a high-speed CCD camera. Distances to projected spots are measured by triangulation. The number of pixels is 361 and the measurement range is 800-2000mm. Although the acquired range image is sparse, we think the proposed sensor is adequate for several applications such as robot vision because of its high-speed imaging and compactness. Actually, Popescu et al. [21] showed that even a range image sensor with only 16 points is effective for modeling.

The future work will include application of the sensor to practical problems that need high-speed range imaging.

VI. ACKNOWLEDGMENTS

This work was partly supported by KAKENHI(16700191).

REFERENCES

[1] R.A. Jarvis, A perspective on range finding techniques for computer vision, Trans. PAMI-5, 2, pp.122-139, 1983.

[2] P. Besl, Active, Optical Range Imaging Sensors, Machine Vision and Applications, Machine Vision and Applications, 1, 2, pp.127–152, 1988.

[3] F. Blais, A Review of 20 Years of Ranges Sensor Development, Videometrics VII, Proceedings of SPIE-IS&T Electronic Imaging, SPIE Volume 5013 , pp.62–76, 2003.

[4] For example, Point Grey Research Inc. http://www.ptgrey.com/

[5] T. Kanade, Development of a Video-Rate Stereo Machine, Proc. 1994 ARPA Image Understanding Workshop (IUW'94), pp.549–558, 1994.

[6] J.A. Beraldin, F. Blais, M. Rioux, J. Domey and L. Cournoyer, A video rate laser range camera for electronic boards inspection, Proc. Vision '90 Conference, pp.4-1–4-11, 1990.

[7] K. Sato, A. Yokoyama and S. Inokuchi, Silicon range finder - a realtime range finding VLSI, Proc. Custom Integrated Circuits Conf., 1994.

[8] T. Kanade, A. Gruss and L.R. Carley, A VLSI sensor based rangefinding system, Robotics Research Fifth International Symposium, pp.49-56, 1990.

[9] K. Sorimachi, Active range pattern sensor, J. Robotics & Mechatronics, 1, pp.269–273, 1989.

[10] K. Nakazawa and C. Suzuki, Development of 3-D robot vision sensor with fiber grating: Fusion of 2-D intensity image and discrete range image, Proc. 1991 International Conference on Industrial Electronics, Control and Instrumentation (IECON '91), pp.2368–2372, 1991.

[11] K. Umeda, A Compact Range Image Sensor Suitable for Robots, Proc. 2004 IEEE International Conference on Robotics and Automation (ICRA'04), pp. 3167–3172, 2004.

[12] T. Tsubouchi, S. Takaki, Y. Kawaguchi and S. Yuta, A straight pipe observation from the inside by laser spot array and a TV camera, Proc. 2000 IEEE/RSJ International Conference on Intelligent Robots and Systems(IROS 2000), pp.82–87, 2000.

[13] Y. Miyazaki, A. Ohya and S. Yuta, Obstacle Avoidance Behavior of Autonomous Mobile Robot using Fiber Grating Vision Sensor, Proc. 2000 IEEE International Conference on Industrial Electronics, Control and Instrumentation, pp.1925-1930, 2000.

[14] T. Oggier, R. Kaufmann, M. Lehmann, P. Metzler, G. Lang, M. Schweizer, M. Richter, B. Buttgen, N. Blanc, K. Griesbach, B. Uhlmann, K.-H. Stegemann, C. Ellmers: "3D-Imaging in Real-Time with Miniaturized Optical Range Camera", Proc. of the Opto-Conference, Nurnberg, DE, May, 2004.

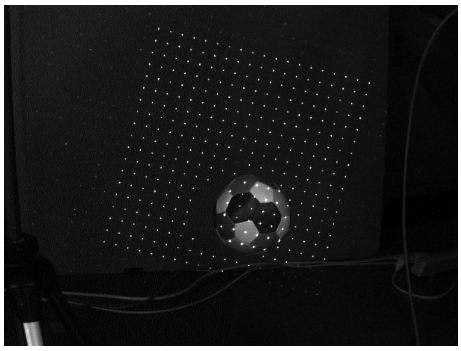

Fig. 11. An experiment to verify 200Hz measurement

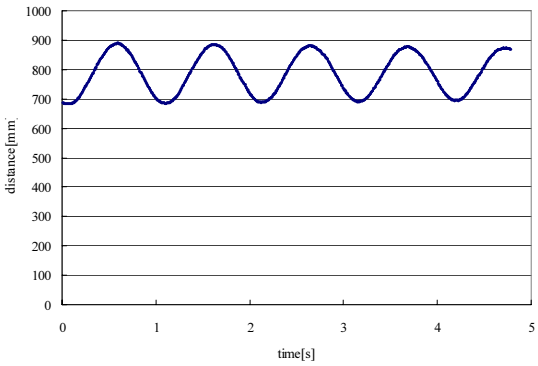

Fig. 12. Center of gravity of the pendulum

[15] S.B. Gokturk, H. Yalcin,and C. Bamji, A Time-of-flight Depth Sensor, System Description, Issues and Solutions, Proc. IEEE Workshop on Real-Time 3D Sensors and Their Use, in conjunction with CVPR, 2004.

[16] I. Ishii, Y. Nakabo, and M. Ishikawa, Target Tracking Algorithm for 1ms Visual Feedback System Using Massively Parallel Processing, Proc. IEEE Int. Conf. Robotics and Automation, pp.2309-2314, 1996.

[17] R. Okada et.al., High-speed object tracking in ordinary surroundings based on temporally evaluated optical flow, Proc. 2003 IEEE/RSJ Int. Conf. on Intelligent Robots and Systems (IROS2003), pp.242–247, 2003.

[18] O. Faugeras, Three-Dimensional Computer Vision, MIT Press, 1993.

[19] R. Baribeau and M. Rioux, Influence of speckle on laser range finders, Appl. Opt., 30(20), pp.2873–2878, 1991.

[20] StockerYale, Inc. http://www.stockeryale.com/

[21] V. Popescu, E. Sacks, and G. Bahmutov, The ModelCamera: a hand-held device for interactive modeling, Proc. Fourth Int. Conf. on 3-D Digital Imaging and Modeling (3DIM 2003), pp.285–292, 2003.

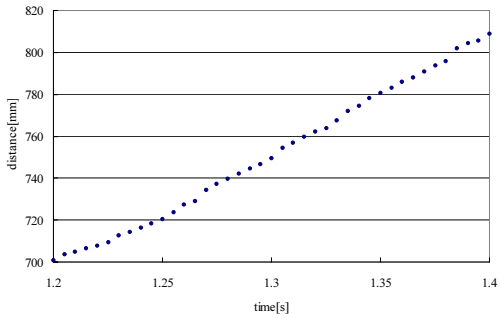

Fig. 13. 1.2∼1.4s of Fig.12

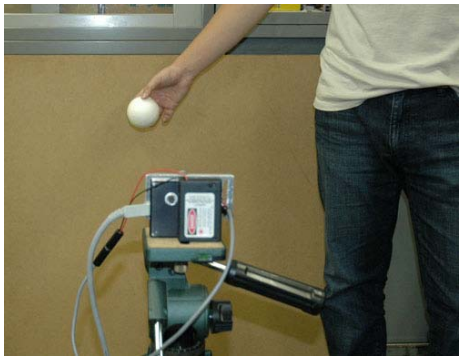

Fig. 14. Scene of measuring a falling ball with the constructed sensor

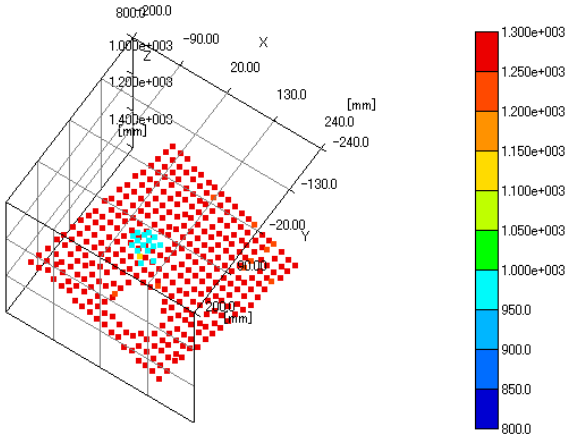

(a)24 frame

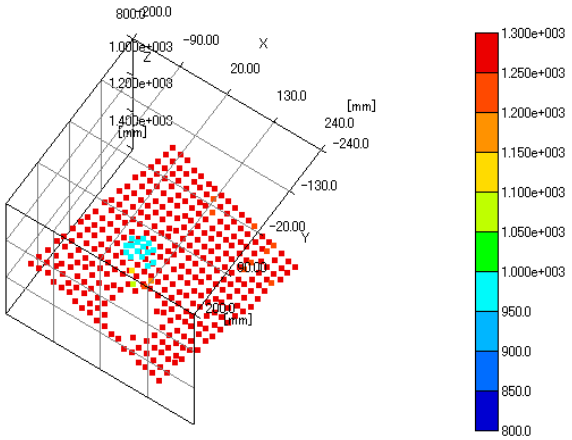

(b)25 frame

Fig. 15. Measurement of a falling ball